



**OPTICAL PARAMETRIC OSCILLATION IN  
ORIENTATION-PATTERNED GALLIUM ARSENIDE**

THESIS

Scott A Shell, Captain, USAF

AFIT/GMS/ENP/07-01

**DEPARTMENT OF THE AIR FORCE  
AIR UNIVERSITY**

***AIR FORCE INSTITUTE OF TECHNOLOGY***

---

**Wright-Patterson Air Force Base, Ohio**

APPROVED FOR PUBLIC RELEASE; DISTRIBUTION UNLIMITED

The views expressed in this thesis are those of the author and do not reflect the official policy or position of the United States Air Force, Department of Defense, or the United States Government.

AFIT/GMS/ENP/07-01

OPTICAL PARAMETRIC OSCILLATION IN  
ORIENTATION-PATTERNED GALLIUM ARSENIDE

THESIS

Presented to the Faculty

Department of Engineering Physics

Air Force Institute of Technology

Air University

Air Education and Training Command

In Partial Fulfillment of the Requirements for the

Degree of Master of Science (Materials Science)

Scott A Shell

Captain, USAF

March 2007

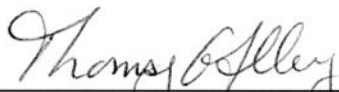
APPROVED FOR PUBLIC RELEASE; DISTRIBUTION UNLIMITED

AFIT/GMS/ENP/07-01

OPTICAL PARAMETRIC OSCILLATION IN  
ORIENTATION-PATTERNED GALLIUM ARSENIDE

Scott A Shell  
Captain, USAF

Approved:

  
\_\_\_\_\_  
Thomas G. Alley (Chairman)

14 Mar 2007  
Date

  
\_\_\_\_\_  
Rita D. Peterson (Member)

15 Mar 07  
Date

  
\_\_\_\_\_  
Matthew J. Bohn (Member)

14 Mar 07  
Date

***Abstract***

Tunable laser sources in the mid-infrared (MIR) spectral range are required for several Air Force applications. Existing lasers with output in the near-infrared can be converted to more desirable MIR by using nonlinear effects. Orientation patterned gallium arsenide (OPGaAs) is a promising nonlinear conversion material because it has broad transparency and can be engineered for specific pump laser and output wavelengths using quasi-phase matching techniques. This research examines optical parametric oscillation (OPO) of several OPGaAs samples using a 2.052  $\mu\text{m}$  wavelength Tm, Ho:YLF pump laser. Of the seven samples available the five that were capable of getting OPO output with this pump were tested and OPO was successfully demonstrated on 4 of the 5. The highest slope efficiency of 10% was seen in sample 5. The highest pump power of incident 190 mW without causing damage to the AR coatings was applied to sample 4. Finally spectroscopic data of input and output was obtained and compared to calculated values.

## *Acknowledgements*

Many thanks are in order to those people who assisted in this endeavor. First and foremost I want to sincerely thank my research sponsor, Dr. Rita Peterson, whose guidance, encouragement, and expertise allowed me to successfully complete this program.

Additionally, I wish to express my appreciation to my faculty advisor, Lt Col Thomas Alley, for his insight, direction, and thoughtful discourse. All of which was very helpful in my research efforts and the composition of my thesis

I also would like to acknowledge the support of Northrop-Grumman Corp. and BAE Systems Inc. through the CARMA effort (F33615-02-2-1111 and F336715-02-2-1110), for providing the samples used in my research.

I would also like to thank my dog Karma for putting up with me cursing at my computer when things didn't always go as planned. Like all dogs she doesn't understand that I'm not angry at her; she merely recognized the anger.

Scott A Shell

## *Table of Contents*

	Page
Abstract .....	v
Acknowledgements .....	v
Table of Contents .....	vi
List of Figures .....	vii
List of Tables .....	viii
I. Introduction .....	1
1.1 Motivation .....	1
1.2 Nonlinear Optical Review .....	2
1.3 Power and Gain Considerations .....	4
1.4 Fabrication .....	8
II. Previous Work .....	10
III. Experimental .....	14
3.1 Pump Laser, 2.052 $\mu\text{m}$ .....	14
3.2 OPG Experiment .....	17
3.3 OPO Experiment .....	19
IV. Results and Discussion .....	24
4.1 Threshold and Slope Efficiency .....	24
4.2 Spectral Data .....	27
V. Conclusions and Recommendations .....	32
Bibliography .....	33

## *List of Figures*

Figure	Page
1.1. Signal and Idler wavelength for OPGaAs versus period given .....	4
1.2. (a) is a schematic showing a singly resonant oscillator and (b).....	6
1.3. OPGaAs Growth Process .....	9
3.1. Pump laser Schematic (Meyer, 2006).....	15
3.2. Beam profile taken with an infrared camera.....	16
3.3. Schematic of the OPG Experiment Setup.....	18
3.4. OPO cavity showing how sample is mounted. The input mirror.....	20
3.5. Schematic of table setup showing OPGaAs OPO setup. ....	22
4.1. Slope efficiency curves for samples 4, 5, 6, and 7.....	26
4.2. Pump spectrum was used to calibrate the monochromator and.....	28
4.3. Signal spectra for each of the samples and gratings. ....	28
4.4. Idler spectra each of the samples and gratings.....	29
4.5. Calculated 2.052 micron quasi-phase matching curves and peak.....	29



## *List of Tables*

Table	Page
2.1. Sample Description .....	12
2.2. Scattering, Absorption and Losses.....	13
4.1. Slope efficiency data for each of the samples and periods .....	25
4.2. Comparison between calculated signal/idler and measured signal/idler .....	30

# OPTICAL PARAMETRIC OSCILLATION IN ORIENTATION-PATTERNED GALLIUM ARSENIDE

## *I. Introduction*

### **1.1 Motivation**

Mid-IR tunable laser output is especially desirable for uses such as infrared counter measures and battlefield remote sensing technologies. Orientation patterned gallium arsenide (OPGaAs) is developing into a promising material for use as an optical parametric oscillator (OPO) to create a tunable source in the mid infrared region, and in the longwave (8-12 $\mu$ m) region as well. Though this material does appear to be a viable candidate for OPO there have been significant challenges in its development. As a semiconductor, GaAs is very well understood; it has been used for many years, it is readily available, and there are numerous established techniques to manufacture GaAs. It also has a desirable transparency window from 1- $\mu$ m to 16  $\mu$ m as well as a high damage tolerance which is an especially desirable characteristic in military applications. It also has a high second order nonlinear coefficient compared to other materials in similar applications. For example OPGaAs has a  $d_{\text{eff}} = 110\text{pm/V}$  versus ZGP which has a  $d_{\text{eff}} = 70\text{ pm/V}$ . (Feijer, 2004)

Unlike many OPO materials OPGaAs is not birefringent. Thus the Poyinting vector does not experience walk off typical in other materials that have been considered

for this application. Unfortunately since it is isotropic it cannot be phasematched using birefringence, and must instead rely on quasi-phasematching (QPM) using a periodic structure. The periodic domains required to generate OPO through QPM in  $\text{LiNbO}_3$  can be generated by applying an electric field across a sample patterned using standard photolithographic techniques. Since GaAs is not ferroelectric several other methods have been explored. One of these methods involved placing a series of GaAs plates at Brewster's angle, (Schlossberg, 1976), and another of them involved manually polishing, slicing and stacking GaAs pieces (Gordon, 1993). Both of these processes yielded nonlinear conversion in a single-pass process, but resulted in too much loss at the domains to be useful in OPO. The process that appears to have the most promise and is in current use is to employ a combination of molecular beam epitaxy (MBE), photolithography, and hydride vapor phase epitaxy (HVPE) to create samples with a periodically patterned thickness greater than 500- $\mu\text{m}$ .

## **1.2 Nonlinear Optical Review**

There are a number of resources available on theories of nonlinear optical processes including optical parametric generation or oscillation and quasi-phase matching. A second order nonlinear process, such as in OPG/OPO, can be defined as an interaction among three photons. In an OPG/OPO, the pump photons have the highest energy and are input into the nonlinear crystal; the other two photons are defined as signal and idler photons and are lower in energy. Frequency conversion occurs when two conditions are met, conservation of energy and conservation of momentum. A pump

photon with an electromagnetic frequency,  $\omega_p$ , generates a signal frequency,  $\omega_s$ , and an idler frequency,  $\omega_i$ , which must satisfy the following energy conservation relationship:

$$\hbar\omega_p = \hbar\omega_s + \hbar\omega_i \quad (1)$$

And since the  $\hbar$  is in all terms it can be canceled and the equation can be simplified:

$$\omega_p = \omega_s + \omega_i \quad (2)$$

In optical parametric generation the pump photons split into signal and idler photons without a second input.

In an OPG/OPO, system, the photons needed for the signal and idler are already present in the form of quantum fluctuations. The photons will attempt to radiate at all frequencies in all directions constrained only by energy conservation. The reason all of these frequencies are not observed is because only those frequencies that meet the phase matching condition are favored for optical amplification. (Sutherland, 1996) In order for the momentum to be conserved the following phase matching condition must be met:

$$\Delta\vec{k} = \vec{k}_p - \vec{k}_s - \vec{k}_i = \frac{2\pi n_p}{\lambda_p} - \frac{2\pi n_s}{\lambda_s} - \frac{2\pi n_i}{\lambda_i} \quad (3)$$

Where  $\vec{k}_j$  is the momentum of the pump, signal, or idler photon and the total momentum must be conserved although generally there is a phase mismatch,  $\Delta\vec{k}$ . One way to eliminate the phase mismatch is to assume birefringent phase matching (BPM). This involves using the crystal orientation and polarization directions to make  $\Delta\vec{k} = 0$ . An alternate approach to BPM is quasi-phase matching (QPM) (Armstrong, 1962). QPM reverses the sign of the nonlinear coefficient after odd multiples of the coherence length. This reversal of the sign shifts the polarization response back into phase with the pump beam which allows for a continued net positive energy flow from the pump into the

signal and idler frequencies. For 1<sup>st</sup> order QPM the domain period is two times the coherence length and the physical distance of each coherence length,  $l_{coh}$ , is defined by:

$$l_{coh} = \frac{\pi}{k_p - k_s - k_i} \quad (4)$$

Although the reversing of the  $d_{eff}$  is effective in ensuring the nonlinear interaction grows it is not quite as efficient as BPM. By knowing these relations it is possible to determine the period that is required to achieve QPM given a particular pump frequency and nonlinear material. This is shown in Figure 1.1 for a couple of given pump wavelengths in OPGaAs.

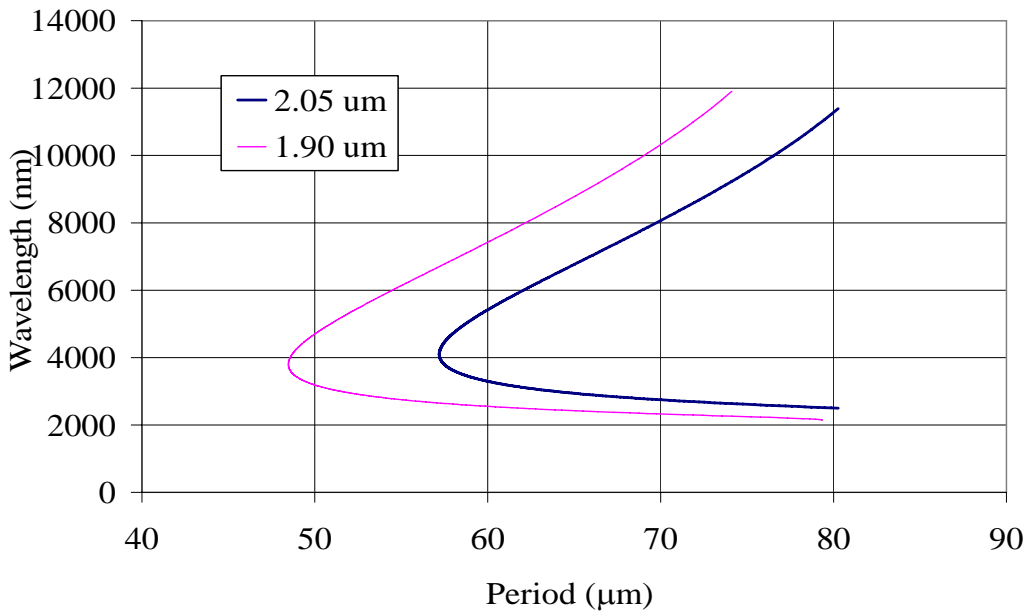


**Figure 1.1. Signal and Idler wavelength for OPGaAs versus period given for two different pump wavelengths, 2.05 micron and 1.90 micron. (Smith, 2005)**

### 1.3 Power and Gain Considerations

Optical Parametric Generation (OPG) is a quantum effect, but since there is a very high number of pump photons it can be treated semi-classically and the pump may be approximated by a constant classical field. Then the signal and idler fields are initially

quantized as  $\frac{1}{2}$  a photon present per mode or alternatively the one photon can be put into the signal and no photon is placed in the idler. By this approach the gain can be calculated and provides the same results as the full quantum mechanical treatment.

The gain equation for a single pass is then shown to be:

$$G_s(L) = \frac{2\omega_s \omega_i d_{eff}^2 I_p}{n_s n_i n_p \epsilon_o c^3} L^2 \frac{\sin^2(\Delta k \cdot L)}{(\Delta k \cdot L)^2} \quad (5)$$

Where L is the overall length of the QPM portion of the nonlinear crystal and  $I_p$  is the pump intensity in  $W/m^2$ . (Harm, 2002) Optical parametric Generation is a spontaneous process and will occur under all conditions. Unfortunately the input pump must be sufficient to create enough output to be measurable and will be explored more in section 3.2 of this document.

In contrast with the single pass OPG process, in an OPO either the signal, the idler, or the signal and idler are resonant in a cavity similar to a laser cavity, though not the same, in that the initial mirror will reflect either the signal or signal and idler completely and the second surface will have a lower reflectance (e.g. 80%) with respect to the signal or signal and idler. The OPO process is a very effective manner in which to increase the net gain of the signal and idler. The signal and idler frequencies will adjust via phase matching to maximize the gain such that these frequencies will achieve the lowest threshold and will be selectively amplified. Several things affect the output frequencies including, but not limited to, the temperature of the crystal, the bandwidth of the pump, and in the presence of birefringence the angle incident on the crystal. In an OPO, unlike in a laser, the signal and idler are only amplified when traveling in the same direction as the pump laser. There are basically two types of OPOs: a singly resonant

oscillator and a doubly resonant oscillator. An OPO which resonates the signal or idler only is a singly resonant oscillator (SRO); an OPO which resonates the signal and idler is a doubly resonant oscillator (DRO).

As briefly described above a singly resonant process involves a set of at least two mirrors in which the first mirror allows the pump to pass freely into the crystal but completely reflects the signal and idler. The second mirror then only needs to reflect the signal or idler in order for SRO to occur, but may also reflect the pump (Figure 1.2a).

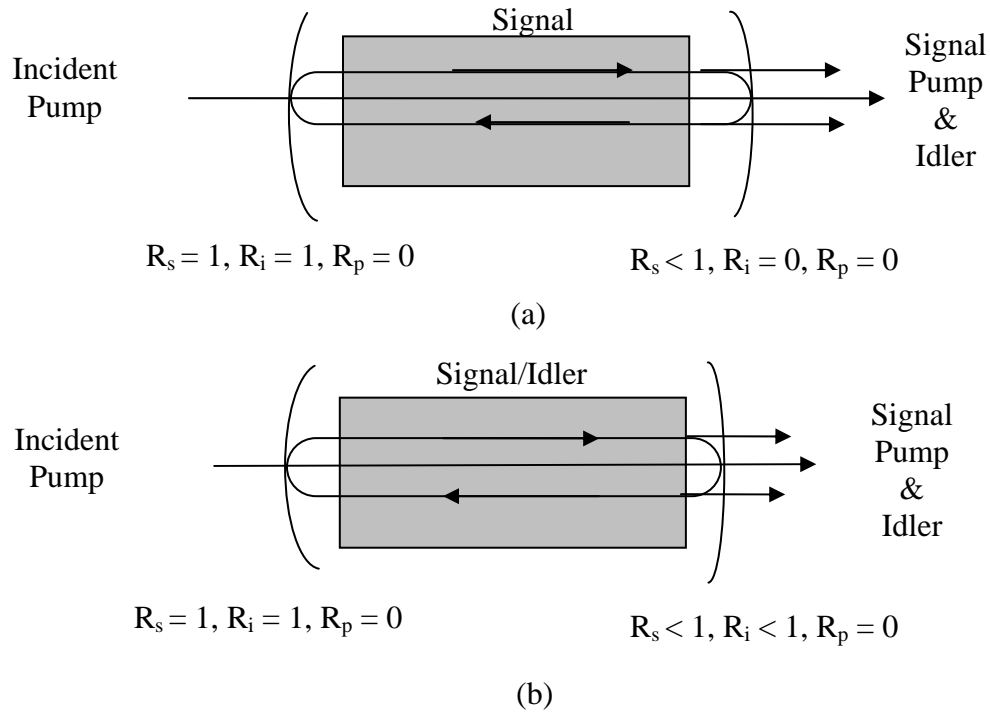


**Figure 1.2. (a) is a schematic showing a singly resonant oscillator and (b) a doubly resonant oscillator.**

If the system is set up as in Figure 1.2a then it can be shown that the pump threshold  $I_{th}$  required to get output in the system will be

$$I_{th}^{SRO} = \left( \frac{\epsilon_o}{\mu_o} \right)^{3/2} \frac{n_s n_i n_p}{2\omega_s \omega_i d_{eff}^2 L^2} \frac{(1 - R_s)}{R_s^2} \quad (6)$$

Where the  $I_{th}$  is the threshold and  $R_j$ , represents the reflectance of the resonator mirrors at the signal and idler wavelengths.

Alternatively in a doubly resonant oscillator the signal and idler are reflected in the resonant cavity. The threshold gain is determined under self-consistent conditions when the parametric gain is equals the round trip electric field loss and similarly to SRO the threshold intensity for DRO can be derived as,

$$I_{th}^{DRO} = \left( \frac{\epsilon_o}{\mu_o} \right)^{3/2} \frac{n_s n_i n_p}{2\omega_s \omega_i d_{eff}^2 L^2} (1 - R_s)(1 - R_i) \quad (7)$$

when the resonator is set up as shown in Figure 1.2(b). Both of these equations assume uniform intensity plane wave interaction but real beams are actually more approximated by Gaussian intensity profiles. Because of this the pump will be focused onto the nonlinear crystal and will not maintain a uniform cross-section over the length of the crystal. Also, the resonated signal and idler beam are not confocal with the pump which will additionally increase the threshold. (Sutherland, 1996)

Also if the SRO threshold is compared to the DRO threshold, the threshold for DRO should be lower than SRO:

$$\frac{I_{th}^{DRO}}{I_{th}^{SRO}} = \frac{(1 - R_i)}{2} \quad (8)$$



Since  $R_i$  must be less than one this equation must also be less than one. For example if the  $R_i = 80\%$  in the DRO system then  $I^{\text{DRO}}/I^{\text{SRO}} = 0.1$ . This is one reason DRO mirrors were used in this experiment. (Yariv & Yeh, 2003)

#### **1.4 Fabrication**

Many nonlinear optical materials are ferroelectric materials and the periodic structures of these materials can be created by applying large voltages thus reversing the sign of the nonlinear coefficient at periodic intervals. Unfortunately, GaAs is not a ferroelectric material and therefore this process is not possible. Early attempts at creating orientation patterned gallium arsenide were by mechanical means.

Thin slices of GaAs were cleaved from hand-polished GaAs wafers; each alternate slice was rotated 180 degrees and then subsequently bonded together. Unfortunately this method resulted in too many imperfections at the interfaces and resulted in the optical losses to be too high to overcome the required threshold for OPO. Later a process was developed to fabricate single crystals of GaAs with periodic regions having alternating domains. This process is summarized in Figure 1.3. Initially the process starts with a GaAs wafer and a thin layer of Germanium (2-3  $\mu\text{m}$ ) is deposited on top of the initial layer of GaAs. Then the Germanium layer was etched, via photolithography, in a periodic pattern (Figure 1.3). It was found that a reversed layer could be formed by using the germanium as an interlayer. After the periodic pattern is created molecular beam epitaxy (MBE) is used to create a lower layer of GaAs of approximately 10  $\mu\text{m}$  thick. MBE is a slow growth process, however, and after this initial growth the remaining thickness is grown by hydride vapor phase epitaxy. HVPE

runs must sometimes be interrupted to allow for removal of parasitic growth on the furnace, after which the sample can be repolished and returned to the furnace for additional growth. This is usually done to grow additional thickness of material, but often produces mixed results. Via this method it has been possible to create samples with periodic structures in excess of 500  $\mu\text{m}$  thick.

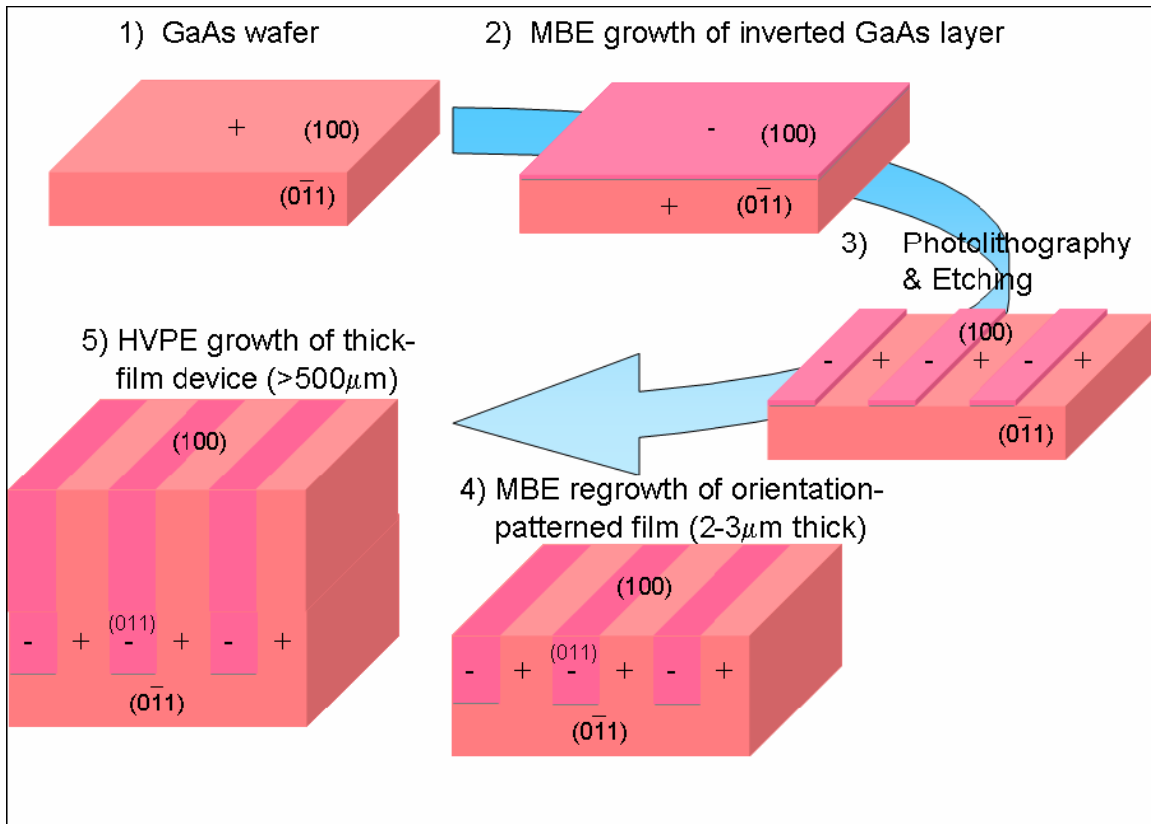


**Figure 1.3. OPGaAs Growth Process**

## ***II. Previous Work***

In 1976 Schlossberg et al attempted to stack a series of GaAs Brewster plates during an early attempt to get frequency doubling with this material. The plates were cut such that the electrical field vector of a CO<sub>2</sub> TEA was parallel to the [111] direction of the crystal. Although his approach is reasonably sound he concluded that the losses due to reflections at the surfaces of the samples were too high for phase matching to occur. (Schlossberg, 1976)

Several years later Gordon et al explored another approach to manufacture GaAs periodic structures for QPM. In order to reduce the losses from the air-semiconductor interface the GaAs layers were diffusion bonded together to create monolithic structures. This process had been used successfully joining dissimilar semiconductors for optoelectronic devices. To do this a variety of lightly doped GaAs wafers were used. They were mechanical grade and polished on both sides. Then the wafers were diced and cleaned thoroughly. They were stacked in a furnace at 840 °C for two hours with a 1 kg weight and an atmosphere of 5% H<sub>2</sub> and 95% N<sub>2</sub>. (Gordon, 1993)

After bonding the samples were cleaved along crystal planes leaving the bonded surfaces intact. Wafers with {110} perpendicular to the surface were chosen because they provided the largest nonlinear coefficient. Again a CO<sub>2</sub> laser was used as the pump laser for the experiment. Gordon et al did several measurements of damage thresholds for these lasers and discovered that although the bulk material seemed to be rather robust but the coatings tended to degrade readily at relatively low pump powers. She also

suggested several structures that would provide promise for tuning output by gradual variations in the thickness of the bonded plates. (Gordon, 1993)

Then in 2002 Harm did several experiments attempting to get QPM OPG and OPO using samples manufactured in a similar process as shown in Figure 1.3. Although ultimately unsuccessful in both respects due to periods that could not be phase matched with the pump laser used he did an exhaustive analysis. He developed a lot of the mathematics that made it easier to understand how OPO in OPGaAs occurs. (Harm, 2002)

Vodopyanov et al then finally demonstrated successful OPO in epitaxially grown OPGaAs. In their system they had a 0.5mm x 5 mm by 11 mm sample with a phase matching period of 61.2  $\mu\text{m}$ . The laser was a Nd:YAG laser pumped OPO tuned between 1.8 and 2  $\mu\text{m}$  with a temperature tuned PPLN Crystal. The experiment primarily explored pump tuning versus signal and idler output wavelengths. (Vodopyanov, 2004)

Then in 2005 Schunemann et al of BAE systems successfully demonstrated OPO in a 62  $\mu\text{m}$  grating. They explored the slope efficiency and surface temperature effects on the output. Their system is more closely related to the system in this study as they used a Tm:Ho:YLF laser pump. Although their pump laser had a slightly different setup their spot size was similar to the work presented here at a radius of 116  $\mu\text{m}$ . The beam had a pulse width of 54 ns although they also explored a pump beam with a pulse width of 25 ns. Their setup did differ from ours in that their output DRO mirrors had 90% reflectance for the signal and idler whereas our output DRO mirrors had an 80% reflectance. (Schunemann, 2005)

Finally Meyer did some very useful work done which allowed a better understanding of the available samples which were manufactured by the process described above (Figure 1.3). The period of the samples ranged from 49  $\mu\text{m}$  to ~64  $\mu\text{m}$  and the thickness of the patterned regions was approximately 0.5 mm. A description of these samples is shown in Table 2.1

**Table 2.1. Sample Description**

Sample	Length	Width	Thickness (including substrate)	Periodicity	Growth Date	Source of Template
	(mm)	(mm)	(mm)	( $\mu\text{m}$ )		
1	5.72	3.89	1.05	62	20 May 04	Stanford
2	7.74	5.42	0.75	49	20 May 04	Stanford
3	13.69	3.84	1.14	49	27 May 04	Stanford
4	10.29	6.07	1.15	62	27 May 04	Stanford
5	16.00	12.40	1.71	62/63/63.8	08 Apr 04	BAE
6	16.00	12.40	1.23	62/63/63.8	18 May 04	BAE
7	17.00	15.00	1.05	61/63	26 May 04	BAE

Meyer did a variety of experiments with the Tm,Ho:YLF laser used in the current research effort and an integrating sphere to characterize the samples in possession but did not go on to demonstrate frequency conversion in any of them (Meyer, 2006). Meyer did excellent characterization of the seven samples which resulted in good scattering, absorption, and loss characteristics for these samples. This data served to determine which samples were the best candidates to use as optical parametric oscillators. The scattering, absorption and loss characteristics are summarized in Table 2.2. For more detailed information about these the losses the reader is directed to Meyer's thesis. (Meyer, 2006) Some of the samples with the lowest overall average losses did have

locations of very high losses. Ultimately there has been a great deal of prior research that has led to the success of this current effort.

**Table 2.2. Scattering, Absorption and Losses**

Sample	Average Total Loss Coef (1/cm)	Standard Deviation	Average Absorption Coef (1/cm)	Standard Deviation	Average Scattering Coef (1/cm)	Standard Deviation
1	1.50	1.00	0.50	0.36	1.0	1
2	1.80	0.20	0.75	0.5	1.1	0.6
3	0.60	0.20	0.50	0.22	0.20	0.1
4	1.20	1.20	0.62	0.6	0.60	1.4
5	0.03	0.03	0.008	0.006	0.02	0.02
6	0.03	0.02	0.01	0.006	0.02	0.02
7	0.60	0.60	0.18	0.14	0.40	0.4

### ***III. Experimental***

As discussed, orientation patterned gallium arsenide (OPGaAs) shows promise as a means of producing radiation across the mid-IR spectral region and into the far-IR as well. The basic scope of this research effort was to demonstrate the capability of either optical parametric generation or optical parametric oscillation (OPO) within the Air Force Research Laboratory, and to compare the various samples provided to us through collaborations with industry.

Experiments in this research were set up similarly to previous experiments performed in the Air Force Research Laboratory (Harm, 2002 and Meyer, 2006). The complete experimental setup and subsequent results will be discussed in the following sections.

#### **3.1 Pump Laser, 2.052 $\mu\text{m}$**

For this experiment the pump wavelength was 2.052  $\mu\text{m}$  and was generated by a laser-diode-pumped, thulium-holmium-doped yttrium lithium fluoride (Tm,Ho:YLF) laser. The laser diode pump was a water-cooled 15 W array of continuous wave aluminum gallium arsenide (AlGaAs) emitters producing a coherent source at 793 nm through a 1 meter length optical fiber shown in figure 3.1. The output was then coupled through a pair of antireflective coated 6 cm focal length lenses into a liquid nitrogen cooled 5x5x5 mm<sup>3</sup> Tm,Ho:YLF crystal with concentrations of Tm and Ho of 6% and 1%, respectively. The side facing the diode laser was AR-coated for 793 nm to transmit

the diode and highly reflectively (HR) coated for  $2.052\ \mu\text{m}$  thus acting as the input (planar) side for a plano-convex laser cavity  $22.4\ \text{cm}$  in length. The outcoupler mirror has a radius of curvature of  $1\ \text{m}$  with a  $70\%$  reflectivity at  $2\text{-}\mu\text{m}$ . The laser was pulsed with a water cooled acousto-optic Q-switch capable of repetition rates from  $100\ \text{Hz}$  to  $10\ \text{kHz}$ , and was operated at  $500\ \text{Hz}$  for these experiments, producing a pulse width of approximately  $40\ \text{ns}$  with an input current to the pump diode array of  $17\ \text{Amps}$ .

At this pump power level, the  $\text{Tm,Ho:YLF}$  laser produced about  $1.5\ \text{W}$  of average power, far in excess of the damage threshold of the OPGaAs samples, In order to attenuate the power incident upon the sample, a half-wave plate was placed before the polarizing component of a faraday isolator which allowed for precise control of the laser power. Following the isolator the laser was turned using a silver mirror then passed through a  $10\text{-cm}$  focal length lens to focus the beam onto the OPGaAs sample.

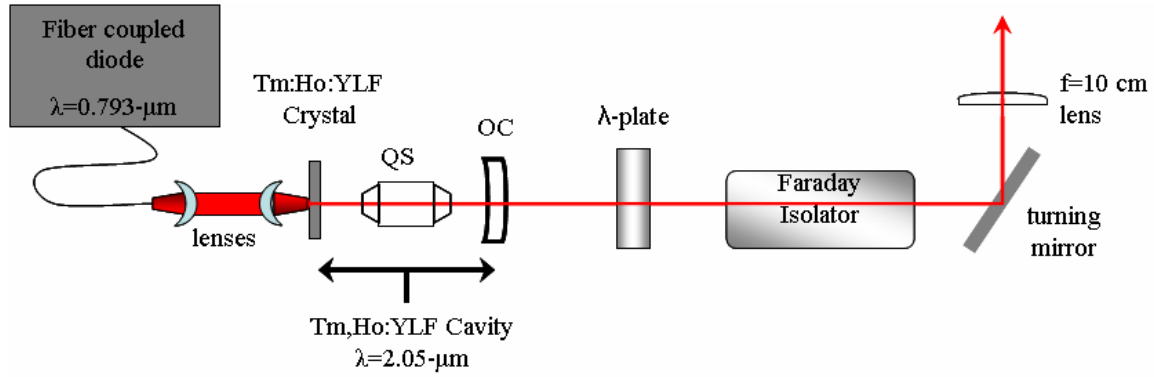


**Figure 3.1. Pump laser Schematic (Meyer, 2006)**

Before attempting to pump samples, the beam profile after the  $10\ \text{cm}$  lens was measured with a Nanoscan beam profiling system to confirm that the beam was similar to the previous experiments: small enough to pass cleanly through the aperture of the patterned area, and to ensure sufficient intensity for efficient nonlinear conversion. The



beam profile was not measured exhaustively but was quickly examined, without a sample in place, and was found to have a focal point at 13.6 cm from the 10 cm lens without the sample present and a radius of about  $80\text{ }\mu\text{m}$  which was consistent with previous experiments. In addition to using the Nanoscan the laser was directed into an IR camera to get an idea of what the pump beam quality was visually (Figure 3.2).

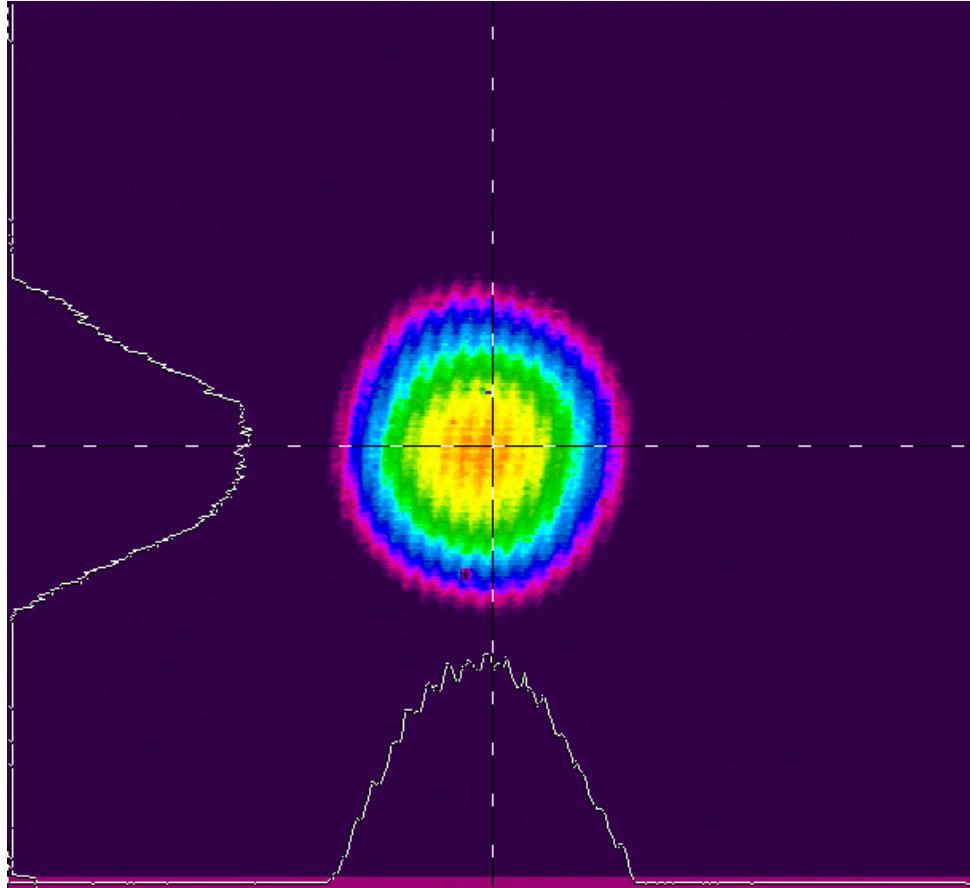


**Figure 3.2. Beam profile taken with an infrared camera.**

Finally, since the OPG/OPO output efficiency can be increased by narrowing the linewidth a “legacy” etalon was installed in the laser cavity and a Spex 220M monochromator was used to determine if narrowing was evident. Unfortunately the etalon did not appear to have substantial effect on the pump laser linewidth and the

linewidth was measured to have a full width half max of 4 nm. This was expected to be sufficiently narrow given that the calculated phase matching bandwidth for this interaction is approximately 4 nm. The output threshold and intensity could be improved by narrowing the frequency of the beam, but it is possible to phase-match using the laser as it is set up.

### **3.2 OPG Experiment**

Before installing resonator mirrors it was thought that an attempt should be made to do Optical Parametric Generation (OPG). This is essentially modeled as a single pass optical parametric process and the setup effectively involves passing the laser through the sample and measuring output. The center grating of sample 5 was chosen for this portion of the experiment as it appeared to have the lowest losses (Table 2.2). Sample 5 is also one of the longer samples and was about 16 cm in length.

In order to ensure that the beam was passing straight through the sample without clipping or total internal reflection, an Electrophysics IR camera was used to view the beam transmitted by the sample. Then to determine if measurable OPG was present a room temperature HgCdTe detector was placed in the beam path on the other side of a longpass filter designed to block the 2.052  $\mu\text{m}$  pump but transmit any signal and idler output. After the unsuccessful attempt to see the output with the room temperature HgCdTe detector a cooled HgCdTe detector was used. This detector was supposed to have a higher sensitivity but unfortunately the electrical noise introduced by the available amplifier was too large to get usable measurements. Finally a high sensitivity Laser

Probe power meter was placed beyond the filter with the intention of measuring signal and idler output. Figure 3.3 shows a schematic of the OPG experiment.

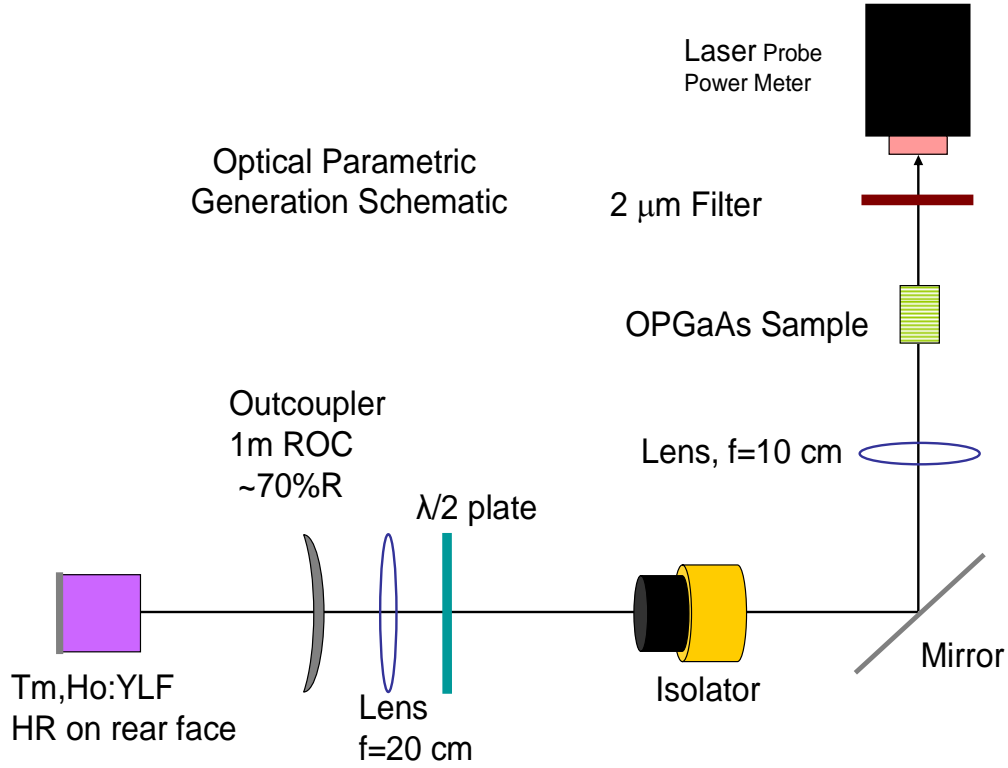


**Figure 3.3. Schematic of the OPG Experiment Setup.**

OPG is a spontaneous process such that when a  $2.052\ \mu\text{m}$  wavelength beam is passed through an OPGaAs sample a signal and idler will be generated. Unfortunately in order to generate enough photons for measurable output it is likely necessary to apply more pump power than is possible without causing damage to the AR coatings on the sample. Thus optical parametric generation was not successful for the OPGaAs samples available in this experiment.

### 3.3 OPO Experiment

After translating sample 5 looking for OPG proved unsuccessful, the decision was made to set up an OPO resonator in the hopes that the resulting feedback would be sufficient to get over threshold and see measurable signal and idler. To simplify the alignment process, a pair of apertures and a power meter was used to ensure the laser was parallel to the surface of the optical bench. Then the beam path was reverse illuminated with a green alignment laser such that the OPO optics and sample could be aligned visually by means of the back reflections. The green alignment laser in conjunction with a power meter proved very effective in aligning the samples for OPO.

The beam profile in the OPO cavity was modeled using Paraxia software in order to predict what mirror radius of curvature would result in a resonant mode most closely overlapping with the pump beam. In addition, in order to more closely resemble previous experiments by Schunemann et al the distance between the mirrors was set as short as practical, 18 mm for sample 5, sample 6, and sample 7 and 14 mm for sample 1 and sample 4. Additionally these cavity lengths were chosen to increase the number of passes per pulse which also should decrease the threshold. Doubly resonant oscillator (DRO) mirrors were used in the experiment. The reason these mirrors were chosen is two fold. First, there was a greater variety of meniscus DRO mirrors available for the wavelengths needed. Second, OPO should have a lower threshold with DRO mirrors then with SRO mirrors. The input mirror was AR coated for  $2.06\text{ }\mu\text{m}$  and HR coated for  $3.5 - 4.5\text{ }\mu\text{m}$ . The output mirror was HR coated for  $2.06\text{ }\mu\text{m}$  and had an 80% Reflectivity at  $3.5 - 4.5\text{ }\mu\text{m}$ . This was a smaller wavelength region from the DRO experiments performed by BAE Systems but seemed to prove effective in producing signal and idler outputs.

Meniscus mirrors were chosen to avoid defocusing the carefully characterized pump beam.

The samples were set on a bracket attached to an x-y-z stage but nothing was done to cool the samples while the laser was applied. (Figure 3.4) After visual alignment of the sample and OPO mirrors with the green laser, the waveplate in the pump train was adjusted to provide approximately 100 mW average power incident on the OPGaAs sample. This average power was chosen because previous experiments by Schunemann et al had found the damage thresholds for these samples to be  $1.36 \text{ J/cm}^2$  which corresponded to 170 mW average power in our laser. This is well over the anticipated threshold to get OPO output of 20-50 mW.

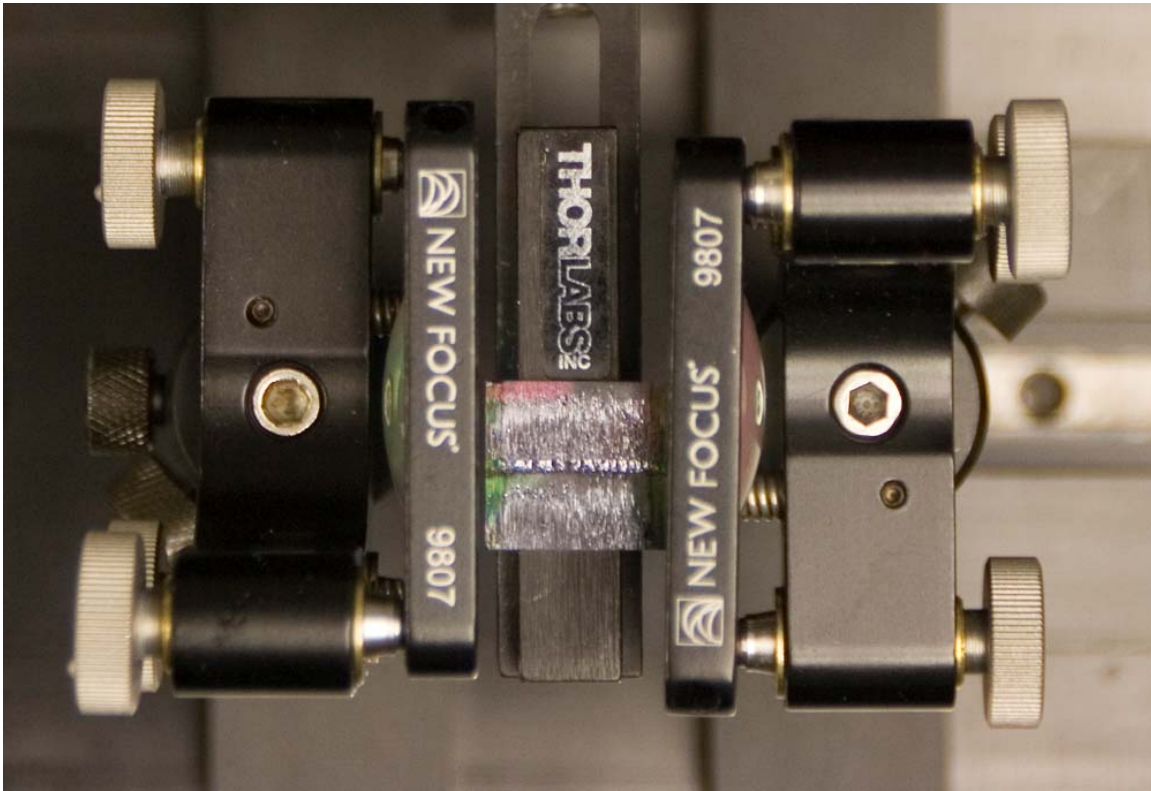


**Figure 3.4. OPO cavity showing how sample is mounted. The input mirror is on the right and the output mirror is on the left.**

To further align the beam through the grating the sample was raised until the sample bracket blocked the input beam. Then the sample was lowered until the power fluctuated at the upper surface, then each of these positions were noted on the z-axis translation stage. The sample was then lowered until the beam diameter was completely within the sample grating. Following this step the sample was translated in order to maximize the power output.

A room temperature HgCdTe IR detector was set up after the 2  $\mu\text{m}$  filter, and the output mirror was adjusted systematically until output was detected. Once a signal and idler were obtained, the detector was removed and replaced with a Laser Probe RM 6600 Universal Radiometer with an RKP-575 sensor head and the input and output OPO mirrors were adjusted to maximize output power. This was done because the HgCdTe IR detector was much more sensitive to the small fluctuations that occur when initially adjusting the mirrors but the threshold of the sensor was far exceeded once OPO was activated. The Newport power meter and Laser Probe power meter were calibrated by measuring power at the same location and produced similar power measurements. During the experiment the incident power was measured with the Newport meter and the output power was measured with the Laser Probe power meter.

Upon getting consistent output with each sample the pump, signal, and idler were directed using mirrors into a monochromator in order to measure the spectral properties of the signal and idler beams (Figure 3.5). The monochromator was a Spex 220M with a 300 and 150 micron grating. The detector was a liquid  $\text{N}_2$  cooled InSb amplified detector. The amplified output of the detector was directed through a Model SR850 DSP lockin amplifier tied to the reference output of the acoustic Q-switch signal generator of

the pump laser. Before directing the laser into the monochromator the beam was passed through optics in order to maximize the coverage on the spectrometer grating, which was a constant struggle throughout the experiment. Calibration of the monochromator was done by measuring the wavelength of the pump beam and making an adjustment within the monochromator software. Although in the interest of completeness of research the pump and signal were measured with the 300 micron grating; all of the results reported in this thesis are from the 150 micron grating since it was capable of measuring the pump, signal, and idler. The resolution of this grating was determined by reflecting the pump laser off of a piece of ground glass into the monochromator then the slit width was decrease until the width of the pump peak didn't change.

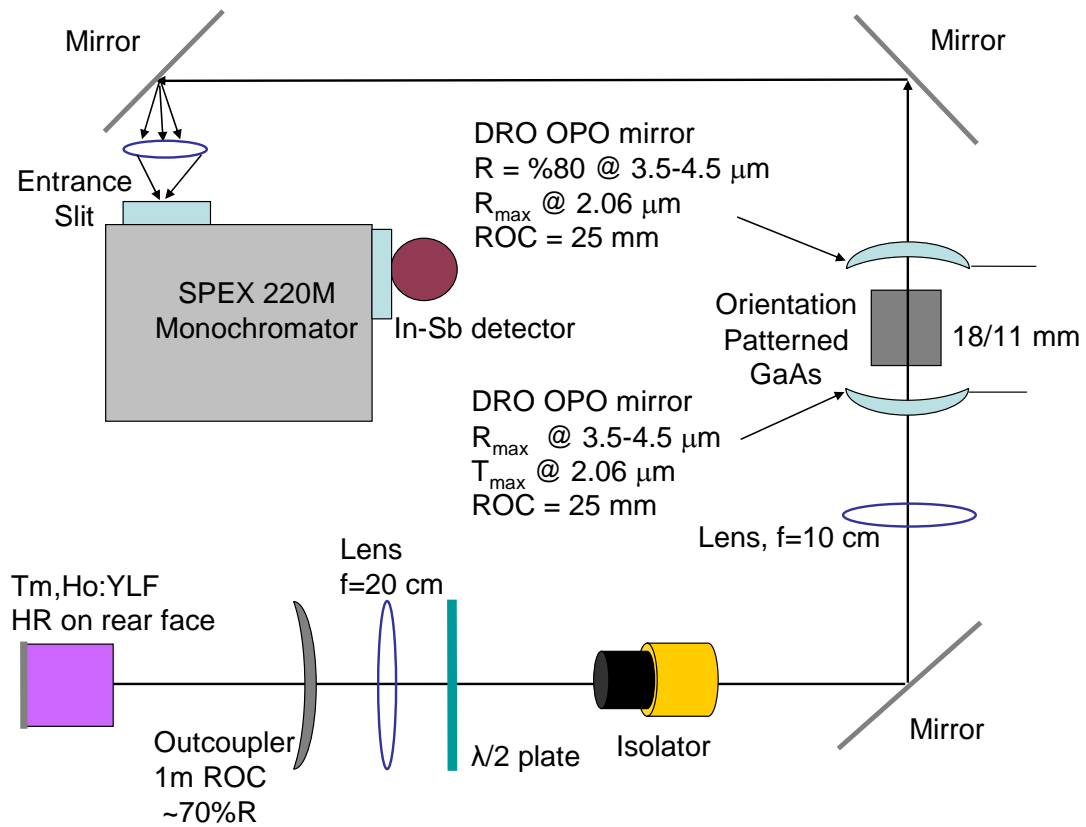


**Figure 3.5. Schematic of table setup showing OPGaAs OPO setup.**

The width of the peak was measured and this value represents the resolution of the laser at a particular slit width. At the slit widths used in the experiment the resolution varied from 10 nm – 20 nm wavelength using slit widths from 0.050 mm – 0.100 mm.



## ***IV. Results and Discussion***

With the 2.052  $\mu\text{m}$  laser, OPO should be possible on samples 1, 4, 5, 6 and 7 based upon phasematching consideration. So far stable OPO has been successfully demonstrated with sample 4, the 62  $\mu\text{m}$  and 63.8  $\mu\text{m}$  gratings of sample 5, the 62  $\mu\text{m}$  grating of sample 6, and both the 61  $\mu\text{m}$  and 63  $\mu\text{m}$  grating of sample 7. Once stable output was obtained with each grating, slope efficiency was measured. Then the pump, signal, and idler were directed into a monochromator and spectral measurements were taken.

### **4.1 Threshold and Slope Efficiency**

The slope efficiency for each sample, and for each grating in the case of the multi-grating samples, was determined by measuring the incident power with a Newport Multifunction optical meter and then measuring the output of the combined signal and idler using a Laser Probe Universal Radiometer.

The input power measurements were all taken immediately following the isolator. Then to calculate the incident power, which is the average power incident on the surface of the sample, the power was measured after the isolator and after the input mirror during the swapping of one of the samples. The average power after the input mirror, of  $90 \pm 1.5$  mW, was then divided by the average power after the isolator, of  $97 \pm 1.5$  mW. Then to convert the input power measurements to incident power the value calculated above was multiplied by the measured input power. The output power was measured after a

filter designed to block the pump but allow the signal and idler to pass freely. This filter was examined in an FTIR and blocked 98% of the pump but allowed all but about 3 – 4% of the signal and idler. This was not accounted for in the calculations.

It appears as though the threshold is generally increasing as the period gets longer, this trend is not entirely consistent as the threshold for the 63  $\mu\text{m}$  period is slightly larger than the 63.8  $\mu\text{m}$  period (Table 4.1). Also, the differences in sample length are expected to have a more significant effect on threshold than the grating period through its influence on signal and idler wavelengths.

**Table 4.1. Slope efficiency data for each of the samples and periods**

Sample #	Period (mm)	% Efficiency	Threshold (mW)
7	61	4.48	$33.63 \pm 0.8$
5	62	11.08	$46.42 \pm 0.8$
6	62	6.36	$47.97 \pm 0.8$
4	62	4.18	$47.53 \pm 0.8$
7	63	5.75	$64.10 \pm 0.8$
5	63.8	10.27	$60.78 \pm 0.8$

The percent slope efficiency tended to be consistent in each sample. Sample 5 had the best slope efficiency of the three samples examined whereas Sample 4 had the worst. This trend appears to be consistent with the loss data found in Table 2.2 collected by Meyer (Meyer, 2006). Sample 5 showed the best transmission and had the highest slope efficiency. Sample 7 did not have quite as good a slope efficiency and the transmission coefficient was lower than sample 5. Sample 4 is the shortest sample and had the lowest slope efficiency. Damage occurred to Sample 1, at a relatively low power of 90-100 mW, before OPO was successfully demonstrated. There did not appear to be a

correlation between the grating periods in each sample and the percent slope efficiency. The slope efficiency merely differed from sample to sample (Figure 4.1).

All of our efficiency values were substantially less than the results from Schunemann et al. Sample 5 which is a sister sample to the one in the BAE experiment doesn't have nearly as high an efficiency as was measured by Schunemann et al. In their experiment they measured a slope efficiency of 20% which is twice what the highest slope reported here is and the remaining samples are much lower. Several factors may have played a part in this. It's possible that our samples had areas with unpatterned gaps causing a reduction in the output efficiency. In addition our laser spot size, pulse width, bandwidth and divergence differed from the BAE setup.

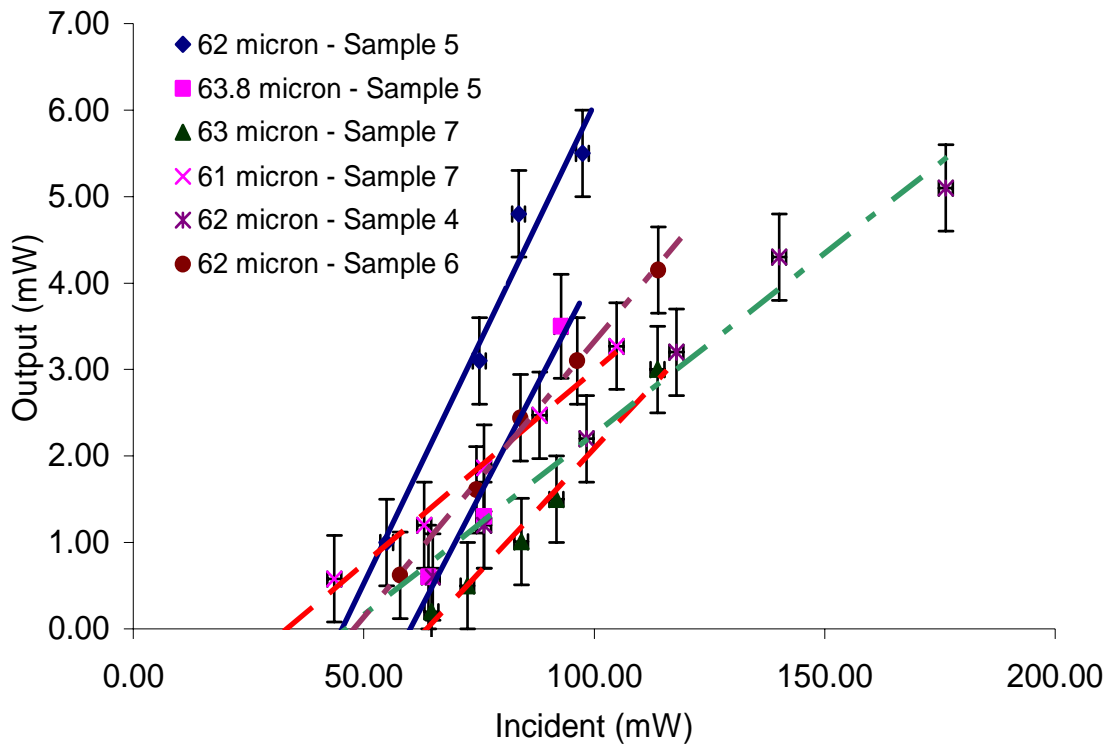


**Figure 4.1. Slope efficiency curves for samples 4, 5, 6, and 7.**

Finally, the BAE DRO output mirror differed substantially from ours in that it reflected 90% of the signal and idler from 3 – 5  $\mu\text{m}$  whereas our DRO output mirror reflected 80% of the signal and idler from 3.5 – 4.5  $\mu\text{m}$ . These effects may have combined to decrease our efficiency. The error for the values of the input and output power was determined through observing the variations in the power as measurements were being taken. Thus these values may include actual deviations in the output in addition to variations in the measuring devices.

## **4.2 Spectral Data**

The most interesting aspect of this experiment was the opportunity to examine the spectral makeup of the signal and idler for each of the samples. For each sample the OPO output was directed into the monochromator and the signal, idler and pump were measured. The pump wavelength was measured primarily in order to calibrate the other results, since the wavelength of the pump laser had been previously established to be 2.052  $\mu\text{m}$  (Figure 4.2). The signal and idler spectra for the various gratings are shown in Figure 4.3 and Figure 4.4. Finally the measured signal and idler were compared to the “calculated” OPO tuning curve for 2.052  $\mu\text{m}$  wavelength. (Figure 4.5)

As is evident from Figure 4.5 the measured peak positions from the signal and idlers for each of the samples are in close agreement to the calculated quasi-phase matched tuning curve. This serves to confirm that the periods of the samples are as they were designed. In addition, the measured signal and idler peak positions as well as calculated values for each sample and grating are shown in Table 4.2.

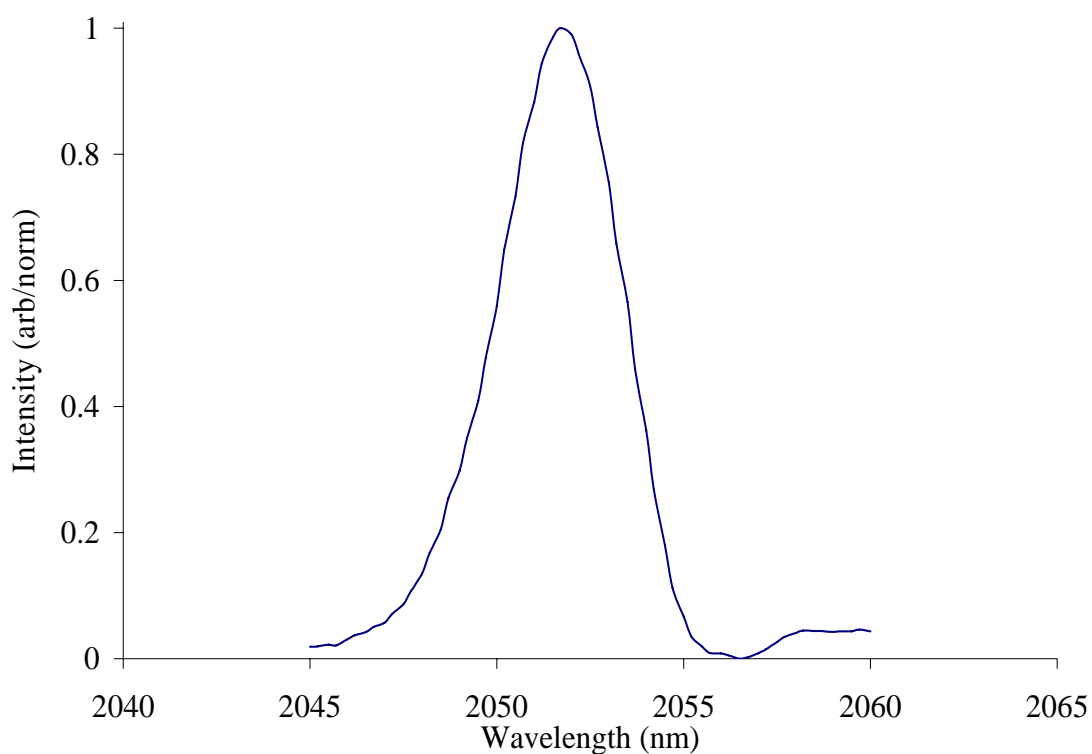


**Figure 4.2. Pump spectrum was used to calibrate the monochromator and is identical for each of the samples.**

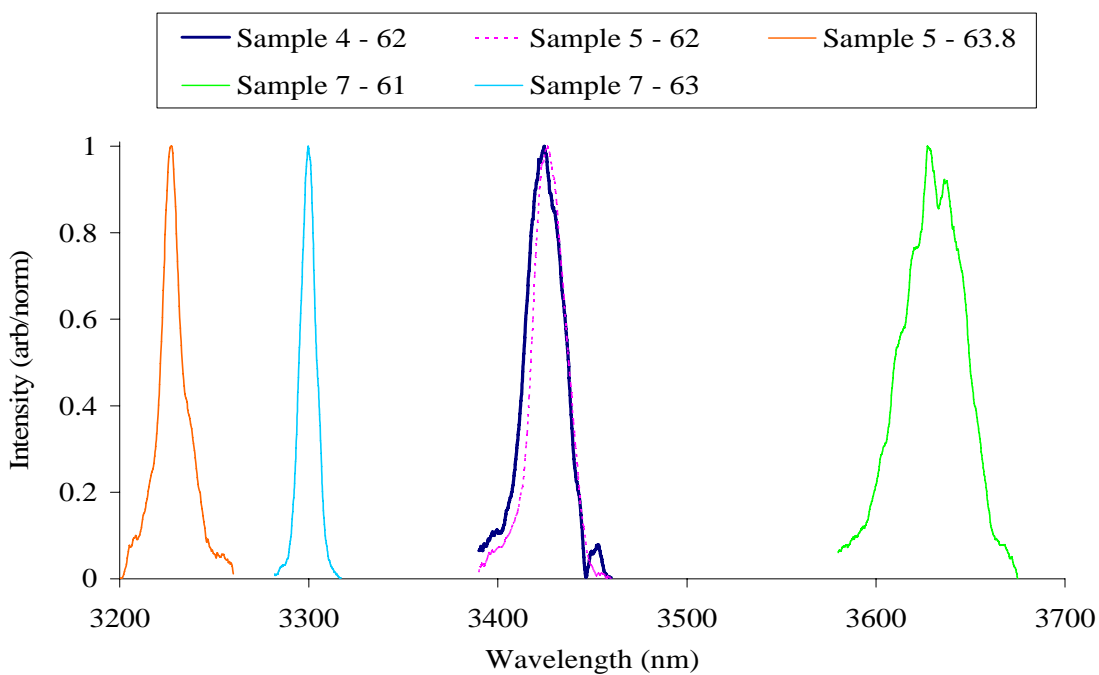


**Figure 4.3. Signal spectra for each of the samples and gratings.**

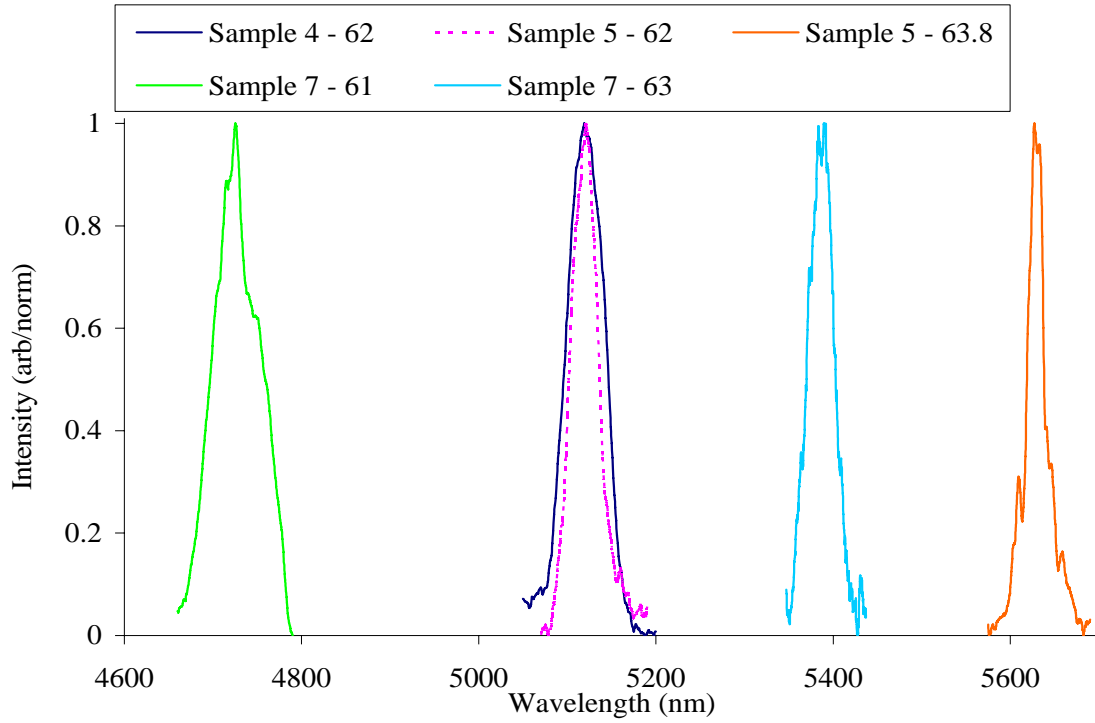


**Figure 4.4. Idler spectra each of the samples and gratings.**

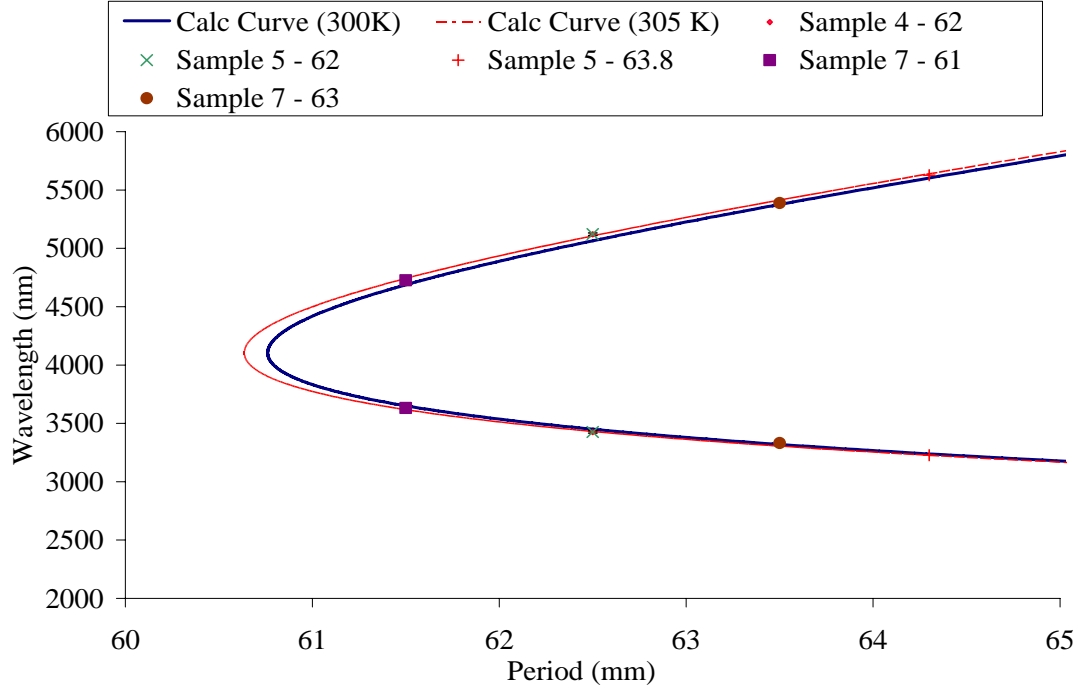


**Figure 4.5. Calculated 2.052 micron quasi-phase matching curves and peak positions for each of the samples and gratings. (Smith, 2006)**

The full width half max of the signal and idler peaks were on the order of 50-100 nm which might account for some of the differences between measured and calculated values, although the actual experimental error is much smaller. Other things that could be causing the variation include thermal effects or slight variations in the period of the samples. Additionally these variations might be due to differences in the values of the index of refraction due to the manufacturing process versus the index of refraction used to calculate signal and idler from the pump. Finally since the sample was not cooled by any means the slight displacement of the measured signal and idler positions might be due to the laser heating up the sample thus causing temperature tuning. In this experiment, a calculated tuning curve based upon a sample temperature of 305 K rather than 300K appears to be slightly closer to the actual measured peak positions.

In this experiment the “calculated” QPM tuning curves were generated using the SNLO program created by Arlee Smith at Sandia National Laboratories.

**Table 4.2. Comparison between calculated signal/idler and measured signal/idler**

Sample	Period	Signal Wavelength (nm)			Idler Wavelength (nm)		
		<i>Calc (RT)</i>	<i>Calc (305K)</i>	<b>Measured</b>	<i>Calc (RT)</i>	<i>Calc (305K)</i>	<b>Measured</b>
4	62	3449	3431	<b>3424.5 ± 10</b>	5065	5104	<b>5120 ± 15</b>
5	62	3449	3431	<b>3426.5 ± 10</b>	5065	5104	<b>5121 ± 15</b>
5	63.8	3239	3227	<b>3227.5 ± 10</b>	5610	5634	<b>5627.2 ± 10</b>
7	61	3651	3617	<b>3631 ± 15</b>	4686	4742	<b>4726 ± 20</b>
7	63	3333	3305	<b>3300 ± 10</b>	5372	5411	<b>5388 ± 20</b>

The error though not substantial was calculated by determining the resolution of the instrument. This was done by reducing the slit diameter while measuring the pump in CW reflected off of a ground glass plate. As the slit is decreased the width of the peak also decreases until the resolution of the grating is reached. When measuring the pump

the maximum resolution was reached when the slits were set at 0.050 mm which resulted in a peak width of about  $\pm 8$  nanometers. The signal and idler error were then adjusted based on how much large the slit needed to be to get measurable output. In this experiment the largest slit used to measure the output signal and idler was 0.100 mm effectively doubling the error in those samples.



## ***V. Conclusions and Recommendations***

The basic objective of this research thesis was to successfully demonstrate optical parametric generation or optical parametric oscillation in samples that were examined in previous experiments, and to provide further comparisons among the various samples. An additional goal was to get spectral data for comparison to calculated quasi-phase matched OPO tuning curves which was very successful.

However there are several things that still can and should be done with respect to this research effort. Generating output using a 1.9  $\mu\text{m}$  Ho:YLF pump laser would be very useful in order to examine samples 2 and 3 with gratings of 49  $\mu\text{m}$  which are incapable of generating output with a 2.052  $\mu\text{m}$  laser, and for gathering additional data on the other samples (See figure 1.1). Use of a Cr:ZnSe pump laser, tunable in the 2.3-2.6  $\mu\text{m}$  range, would make it straightforward to spectrally tune the OPGaAs OPO output by tuning the pump laser wavelength. Additionally there is an interest in determining if incorporating an etalon can improve output slope efficiency using the current laser setup. Suffice to say there are a number of very useful directions that this research effort can go.

## ***Bibliography***

- Armstrong, J. A., Bloembergen, N., Ducuing, J., Pershan, P. S., "Interactions between light waves in a nonlinear dielectric," *Physical Rev.*, Vol 127, pp1918-1925, **1962**.
- Fejer, Martin. M., "Orientation Patterned Semiconductors: Growth and Applications," Unpublished Briefing, Stanford, 21 January **2004**.
- Gordon, L., G.L. Woods, R.C. Eckardt, R.R. Route, R.S. Feigelson, M.M Fejer, and R.L. Byer, "Diffusion-bonded stacked GaAs for Quasi-phase matched Second-Harmonic Generation of a Carbon Dioxide laser," *Electronics Letters*, 29, 1942-1944, 28 October **1993**.
- Harm, Michael D., *Development of a Tm:Ho:TLF-Laser-Pumped Orientation-Patterned Gallium Arsenide Optical Parametric Oscillator*, Air Force Institute of Technology (AU), Wright Patterson Air Force Base, OH, March **2002**.
- Meyer, Joshua W., *Optical Characterization of Thick Growth Orientation-Patterned Gallium Arsenide*, Air Force Institute of Technology (AU), Wright Patterson Air Force Base, OH, March **2006**.
- Schunemann, P. G., Setzler S. D., Mohnkern L., and Pollak T. M., "2.05- $\mu$ m-laser-pumped orientation-patterned gallium arsenide (OPGaAs) OPO," *Optical Society of America*, Washington, DC. **2002**.
- Schlossberg, H., Hordvik, A., Szilagyi, A., "A quasi-phase-matching technique for efficient optical mixing and frequency doubling," *Journal of Applied Physics*, Vol 47, No 5. May **1976**.
- Smith, Arlee V., *SNLO nonlinear Optics Code available from A. V. Smith*, Sandia National Laboratories, Albuquerque, NM, 87185-1423, April, **2005**.
- Sutherland, R. L., *Handbook of Nonlinear Optics*, Marcel Dekker, Inc. New York. **1996**.
- Vodopyanov, K. L., Levi, O., Kuo, P. S., Pinguet, T. J., Harris J. S., and Fejer M. M., "Optical parametric oscillation in quasi-phase-matched GaAs". *Optics Letters*. Vol 29, No 16. 15 Aug **2004**.
- Yariv, Amnon. Yeh, Pochi, *Optical Waves in Crystals*, Wiley-Interscience, **2003**.

REPORT DOCUMENTATION PAGE				Form Approved OMB No. 074-0188	
<p>The public reporting burden for this collection of information is estimated to average 1 hour per response, including the time for reviewing instructions, searching existing data sources, gathering and maintaining the data needed, and completing and reviewing the collection of information. Send comments regarding this burden estimate or any other aspect of the collection of information, including suggestions for reducing this burden to Department of Defense, Washington Headquarters Services, Directorate for Information Operations and Reports (0704-0188), 1215 Jefferson Davis Highway, Suite 1204, Arlington, VA 22202-4302. Respondents should be aware that notwithstanding any other provision of law, no person shall be subject to a penalty for failing to comply with a collection of information if it does not display a currently valid OMB control number.</p> <p><b>PLEASE DO NOT RETURN YOUR FORM TO THE ABOVE ADDRESS.</b></p>					
1. REPORT DATE (DD-MM-YYYY) 22-03-2007		2. REPORT TYPE Master's Thesis		3. DATES COVERED (From – To) May 2006 – Mar 2007	
4. TITLE AND SUBTITLE  Optical Parametric Oscillation in Orientation-Patterned Gallium Arsenide				5a. CONTRACT NUMBER	
				5b. GRANT NUMBER	
				5c. PROGRAM ELEMENT NUMBER	
6. AUTHOR(S)  Shell, Scott, A., Captain, USAF				5d. PROJECT NUMBER	
				5e. TASK NUMBER	
				5f. WORK UNIT NUMBER	
7. PERFORMING ORGANIZATION NAMES(S) AND ADDRESS(S) Air Force Institute of Technology Graduate School of Engineering and Management (AFIT/EN) 2950 Hobson Way WPAFB OH 45433-7765				8. PERFORMING ORGANIZATION REPORT NUMBER  AFIT/GMS/ENP/07-01	
9. SPONSORING/MONITORING AGENCY NAME(S) AND ADDRESS(ES)				10. SPONSOR/MONITOR'S ACRONYM(S)	
				11. SPONSOR/MONITOR'S REPORT NUMBER(S)	
12. DISTRIBUTION/AVAILABILITY STATEMENT APPROVED FOR PUBLIC RELEASE; DISTRIBUTION UNLIMITED.					
13. SUPPLEMENTARY NOTES					
14. ABSTRACT Tunable laser sources in the mid-infrared (MIR) spectral range are required for several Air Force applications. Existing lasers with output in the near-infrared can be converted to more desirable MIR by using nonlinear effects. Orientation patterned gallium arsenide (OPGaAs) is a promising nonlinear conversion material because it has broad transparency and can be engineered for specific pump laser and output wavelengths using quasi-phase matching techniques. This research examines optical parametric oscillation (OPO) of several OPGaAs samples using a 2.052 $\mu$ m wavelength Tm, Ho:YLF pump laser. Of the seven samples available the five that were capable of getting OPO output with this pump were tested and OPO was successfully demonstrated on 4 of the 5. The highest slope efficiency of 10% was seen in sample 5. The highest pump power of incident 190 mW without causing damage to the AR coatings was applied to sample 4. Finally spectroscopic data of input and output was obtained and compared to calculated values.					
15. SUBJECT TERMS Optical Parametric Oscillation, Orientation Patterned Gallium Arsenide, Nonlinear Optics,					
16. SECURITY CLASSIFICATION OF:			17. LIMITATION OF ABSTRACT	18. NUMBER OF PAGES	19a. NAME OF RESPONSIBLE PERSON
REPORT U	ABSTRACT U	c. THIS PAGE U			Thomas G. Alley, Lt Col, USAF (ENP)
				43	19b. TELEPHONE NUMBER (Include area code) (937) 255-3636, ext 4649; e-mail: Thomas.Alley@afit.edu